Optimal boundary control for the heat equation with application to freezing with phase change

Christoph Josef Backi[1] **and Jan Tommy Gravdahl**[2]
Department of Engineering Cybernetics
Norwegian University of Science and Technology
O.S. Bragstads plass 2D, 7034 Trondheim, Norway

***Abstract*— In this paper an approach for optimal boundary control of a parabolic partial differential equation (PDE) is presented. The parabolic PDE is the heat equation for thermal conduction. A technical application for this is the freezing of fish in a vertical plate freezer. As it is a dominant phenomenon in the process of freezing, the latent heat of fusion is included in the model. The aim of the optimization is to freeze the interior of a fish block below -18 °C in a predefined time horizon with an energy consumption that is as low as possible assuming that this corresponds to high freezing temperatures.**

I. INTRODUCTION

The system studied in this paper is a model of heat exchange phenomena, known as the heat equation. This is a parabolic partial differential equation (PDE).

General numerical optimization and optimal control have been studied and introduced in a great number of publications, such as [12] and [5]. In [12] an introduction to (un–)constrained optimization and methods to solve either of these problems are given. A detailed overview over numerical tools for solving optimal control problems, both in discrete and continuous time, is provided in [5].

Optimal control of PDEs has been studied in many papers, such as [6], [7], [8] and [1]. In [6] and [7], mathematical aspects are studied, such as rewriting the PDE into a state space form by defining operators. In [8] a detailed overview of theoretical principles for controlling PDEs optimally is presented, as well as an introduction of methods to solve them and applications for the theoretical results. In [1] practical approaches to optimal model predictive control of the heat equation are demonstrated.

The heat exchange phenomenon in this paper is the freezing of a fish block in a vertical plate freezer. The fish is headed and gutted and afterwards filled into the vertical plate freezer (see Fig. 1 left) where it gets frozen as a block (see Fig. 1 right). The cooling medium is liquid ammonia at minimal 235 K, which is forced through the plate freezer by a pump. When taking heat off the fish block, the ammonia partly vaporizes and in a cycle process this added amount of heat gets removed by a compression/condensation/throttling - process. For a schematic of the cycle process see Fig. 2.

Due to the fact that fish consists of a large amount of water, it can be assumed that certain thermodynamical phenomena hold. If water is cooled down below its freezing point one can observe that for a certain period of time the temperature will remain constant at the freezing point. Thus when a phase change occurs (here for water from liquid to solid state) an additional amount of energy has to be removed from the system. This amount of energy is the so called latent heat of fusion. Physically, latent heat of fusion is a hidden amount of energy that is needed to break the grid structure of the solid phase when melting ice. Many researchers have studied this phenomenon in numerical simulations of the heat equation, e.g [11] introduced different schemes for adapting the heat transfer parameters to model latent heat of fusion. In [13] and [14] progresses in the field of modeling freezing processes are described. A review about modeling heat and mass transfer in frozen foods is given in [15].

The overall aim is to freeze the interior of a fish block below -18 °C in a predefined time horizon. The freezing process is supposed to consume as little energy as possible assuming that this corresponds to high freezing temperatures. This assumption leads to the definition of an optimal control problem. To the authors best knowledge, there are no previous results presented in the literature on optimal boundary control of freezing taking latent heat of fusion into account.

Fig. 1. Vertical plate freezer (left) and fish block (right)

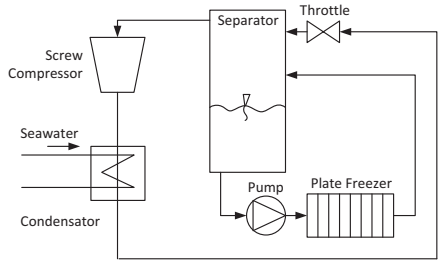

Fig. 2. Freezing process

[1]corresponding author, christoph.backi@itk.ntnu.no
[2]jan.tommy.gravdahl@itk.ntnu.no

II. MODEL

For simplicity, and without loss of generality, only one spatial dimension is considered when choosing the equation that models the freezing process.

A. Model equations

The equation of the parabolic PDE is as follows

$$\rho(T)\,c(T)\,\frac{\partial}{\partial t}T(t,x)=\frac{\partial}{\partial x}\left[\lambda(T)\,\frac{\partial}{\partial x}T(t,x)\right]$$

with

$$\frac{\partial}{\partial x}\lambda(T)=\frac{\partial\lambda(T)}{\partial T}\frac{\partial T(t,x)}{\partial x}=\lambda_T(T)\,\frac{\partial T(t,x)}{\partial x}$$

and thus

$$\rho(T)\,c(T)\,\frac{\partial T(t,x)}{\partial t}=\lambda_T(T)\left[\frac{\partial T(t,x)}{\partial x}\right]^2+\lambda(T)\,\frac{\partial^2 T(t,x)}{\partial x^2} \tag{1}$$

where T denotes the temperature, $\rho(T)$ is the density, $c(T)$ indicates the specific heat capacity at constant pressure, $\lambda(T)$ describes the thermal conductivity and $\lambda_T(T)$ is the derivative of $\lambda(T)$ with respect to the temperature T. The PDE (1) is thus nonlinear.

Note that both ρ, c and λ depend on the temperature T. There are several ways to describe this temperature dependency. One method is to use a step-function and define constant values above and below the freezing point, which is the least accurate approach. Another method is to define continuous functions representing even better approximations to the real parameters. The latter approach is demonstrated in [4] where it is also shown that fish can be considered as a thermodynamical alloy of many substances, such as water, fat, proteins, and so on. Thus, the parameters $\rho(T)$, $c(T)$ and $\lambda(T)$ can be calculated as a sum of the parameters of the actual substances multiplied by their mass-fraction.

To keep notation simple, two new parameters can be introduced as

$$k(T)=\frac{\lambda(T)}{\rho(T)\,c(T)} \tag{2}$$

and

$$k_T(T)=\frac{\lambda_T(T)}{\rho(T)\,c(T)}. \tag{3}$$

This leads to a rewritten form of (1)

$$\frac{\partial}{\partial t}T(t,x)=k_T(T)\left[\frac{\partial}{\partial x}T(t,x)\right]^2+k(T)\,\frac{\partial^2}{\partial x^2}T(t,x), \tag{4}$$

or, with simpler notation,

$$T_t=k_T(T)\,T_x^2+k(T)\,T_{xx}. \tag{5}$$

B. Latent heat of fusion

As mentioned before, the phenomenon of latent heat of fusion has to be modeled explicitly. This can be done by using an approach described in [11] named the *apparent heat capacity method* where the parameters $c(T)$ and $\lambda(T)$ are defined as follows

$$c(T)=\begin{cases}c_s, & T<T_f-\Delta T\\ \frac{c_l+c_s}{2}+\frac{LH}{2\Delta T}, & T_f-\Delta T\le T\le T_f+\Delta T\\ c_l, & T>T_f+\Delta T\end{cases} \tag{6}$$

$$\lambda(T)=\begin{cases}\lambda_s, & T<T_f-\Delta T\\ \lambda_s+\frac{(\lambda_l-\lambda_s)\left[T-\left(T_f-\Delta T\right)\right]}{2\Delta T}, & T_f-\Delta T\le T\le T_f+\Delta T\\ \lambda_l, & T>T_f+\Delta T.\end{cases} \tag{7}$$

The index s denotes solid state and the index l denotes liquid state, respectively. LH indicates the amount of latent heat of fusion, ΔT is a temperature interval around the freezing point temperature T_f. The size of ΔT influences how long it takes until the latent heat of fusion is removed from the medium (fish block). Therefore, in practice, this parameter can be chosen to fit a measured freezing curve. Note that $\rho(T)$ is considered to be constant over the whole temperature range.

The chosen approach corresponds to the earlier described definition of parameters with constant values above and below the freezing point. Nevertheless, case defined functions for the parameters (see (6) and (7)) may not necessarily be implementable in any optimization environment. Therefore, $k(T)$ can be approximated by a continuous expression using arctan-functions

$$\begin{aligned}k(T)\approx{}&7\cdot10^{-8}\\ &+2.737\cdot10^{-7}\left[-\arctan\left(\left(\frac{T}{T_f-\Delta T}-1\right)20000\pi\right)+\frac{\pi}{2}\right]\\ &+4.35\cdot10^{-8}\left[\arctan\left(\left(\frac{T}{T_f+\Delta T}-1\right)50000\pi\right)\right].\end{aligned} \tag{8}$$

An approximation is necessary due to the fact that the optimization software intended to use requires a continuous representation for $k(T)$. The values in (8) were found by curve–fitting to approximate the function defined in (2). A comparison between $k(T)$ defined in (2), (6) and (7), and its approximation (8) can be seen in Fig. 3.

Furthermore, the parameter $k_T(T)$ has to be defined and thus approximations for functions (6) and (7) are needed as well. The arctan-function showed itself to be a good decision for approximating the parameter $k(T)$ and thus the following approximations for the parameters $c(T)$ and $\lambda(T)$ have also been found by curve–fitting:

$$\begin{aligned}c(T)\approx{}&-1.374\cdot10^{5}\\ &+8.938\cdot10^{4}\left[\arctan\left(\left(\frac{T}{T_f-\Delta T}-1\right)50000\pi\right)+\frac{\pi}{2}\right]\\ &+8.888\cdot10^{4}\left[-\arctan\left(\left(\frac{T}{T_f+\Delta T}-1\right)50000\pi\right)\right],\end{aligned} \tag{9}$$

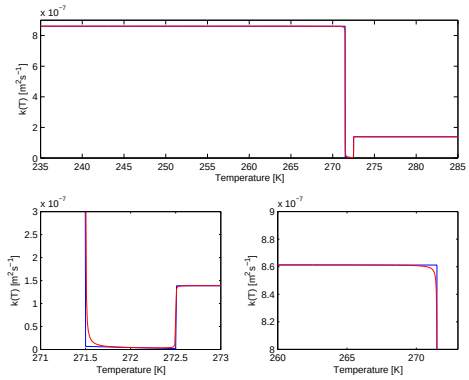

Fig. 3. Parameter $k(T)$ as defined in (2), (6) and (7) (blue) compared to the approximation defined in (8) (red)

whose plot can be seen in Figure 4 compared to original definition in (6) and

$$\lambda(T) \approx 0.49+0.42\left[-\arctan\left(\left(\frac{T}{T_f}-1\right)400\pi\right)+\frac{\pi}{2}\right], \tag{10}$$

whose plot can be seen in Figure 5 compared to original definition in (7).

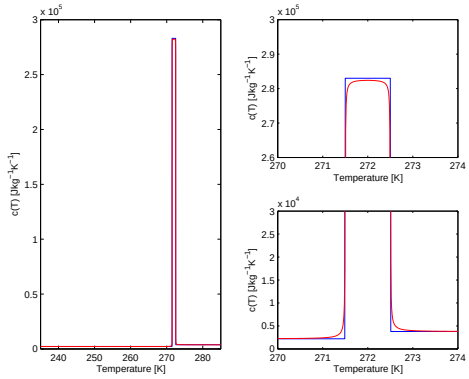

Fig. 4. Parameter $c(T)$ as defined in (6) (blue) compared to the approximation defined in (9) (red)

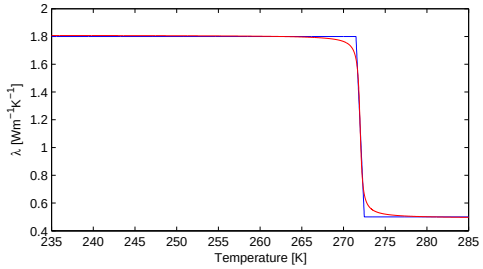

Fig. 5. Parameter $\lambda(T)$ as defined in (7) (blue) compared to the approximation defined in (10) (red)

Differentiating (10) with respect to temperature T gives

$$\lambda_T(T) = \frac{166\pi}{T_f\left(1+160000\pi^2\left(T/T_f-1\right)^2\right)} \tag{11}$$

and thus the parameter $k_T(T)$ defined in (3) can be calculated with the functions defined in (9) and (11). Its plot can be seen in Figure 6.

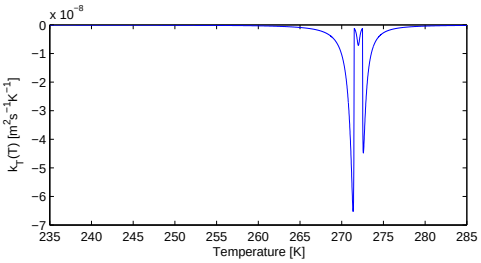

Fig. 6. Parameter $k_T(T)$ as defined in (3)

Note that for all plots of the approximated parameters the values $T_f = 272$ K and $\Delta T = 0.5$ K were used.

C. Boundary and initial conditions

The Dirichlet boundary conditions represent the input to the system, meaning that they are functions of temperature depending on time: $T(t,0) = T(t,L) = u(t)$. Here L denotes the length of the fish block and $u(t)$ is the input function over time.

The initial condition is chosen to be evenly distributed over the whole spatial variable: $T(0,x) = T_{init}$.

D. Discretization

The model can be discretized in time and space. But again, in the interest of simplicity, it will only be discretized in space and not in time. This approach leads to a manageable amount of states and leaves the time-discretization to the optimization software. Thus a set of continuous ordinary differential equations (ODEs) constrains the optimization problem.

The discretization in space is done by a forward difference approach and a center difference approach, respectively

$$\frac{\partial^2}{\partial x^2}T = \frac{T_{n+1}-2T_n+T_{n-1}}{\Delta x^2}$$
$$\left[\frac{\partial}{\partial x}T\right]^2 = \frac{T_{n+1}^2-2T_{n+1}T_n+T_n^2}{\Delta x^2}$$

where the time dependency of the temperature T is not explicitly shown. Further Δx describes the spatial resolution, meaning that $\Delta x = \frac{L}{N}$, where N denotes the number of cells. Thus the running variable is defined as $1 \leq n \leq N$.

After discretization and introduction of the boundary conditions, (4) can be rewritten to

$$\begin{aligned}
\dot{T}_1 &= \frac{k_T(T_1)}{\Delta x^2}\left[T_1^2 - 2T_1 u + u^2\right] + \frac{k(T_1)}{\Delta x^2}\left[T_2 - 2T_1 + u\right] \\
&\vdots \\
\dot{T}_n &= \frac{k_T(T_n)}{\Delta x^2}\left[T_{n+1}^2 - 2T_{n+1}T_n + T_n^2\right] \\
&\quad + \frac{k(T_n)}{\Delta x^2}\left[T_{n+1} - 2T_n + T_{n-1}\right] \\
&\vdots \\
\dot{T}_N &= \frac{k_T(T_N)}{\Delta x^2}\left[u^2 - 2uT_N + T_N^2\right] + \frac{k(T_N)}{\Delta x^2}\left[u - 2T_N + T_{N-1}\right]
\end{aligned} \tag{12}$$

meaning that a set of N coupled, nonlinear ODEs is obtained where $T \in \mathbb{R}^{N_+}$ and $u \in \mathbb{R}^+$.

III. STABILITY

The following stability proof is inspired by [10, Ch. 2] and is based on the PDE itself, not its discretization. The steady state solution for the system (4) is $\overline{T} = u$. An error term is defined as $w(t,x) = T(t,x) - \overline{T} \Rightarrow T(t,x) = w(t,x) + \overline{T}$. After normalizing the length L, (5) can be rewritten as

$$\begin{aligned}
w_t(t,x) + \underbrace{\overline{T}_t}_{=0} &= \frac{k_T\left(w+\overline{T}\right)}{L^2}\left[w_x(t,x) + \underbrace{\overline{T}_x}_{=0}\right]^2 \\
&\quad + \frac{k\left(w+\overline{T}\right)}{L^2}\left[w_{xx}(t,x) + \underbrace{\overline{T}_{xx}}_{=0}\right] \\
\Rightarrow w_t(t,x) &= \frac{k_T\left(w+\overline{T}\right)}{L^2} w_x^2(t,x) + \frac{k\left(w+\overline{T}\right)}{L^2} w_{xx}(t,x).
\end{aligned}$$

Define a Lyapunov function candidate V as the L_2 spatial norm

$$V = \frac{1}{2}\int_0^1 w^2(t,x)\, dx := \frac{1}{2}\|w(t)\|^2. \tag{13}$$

Differentiating (13) with respect to time and not explicitly marking the dependency of k_T and k on $w+\overline{T}$ leads to

$$\begin{aligned}
\dot{V} &= \int_0^1 w(t,x)\, w_t(t,x)\, dx \\
&= \frac{1}{L^2}\int_0^1 \left[k_T\, w(t,x)\, w_x^2(t,x) + k\, w(t,x)\, w_{xx}(t,x)\right] dx.
\end{aligned}$$

Integrating the term $w(t,x)\, w_{xx}(t,x)$ by parts one obtains

$$\begin{aligned}
\dot{V} &= \frac{1}{L^2}\int_0^1 \left[k_T\, w(t,x)\, w_x^2(t,x) - k\, w_x^2(t,x)\right] dx \\
&= \frac{1}{L^2}\int_0^1 \left[k_T\, w(t,x) - k\right] w_x^2(t,x)\, dx.
\end{aligned}$$

Remember that $k_T < 0 \,\forall\, w + \overline{T}$ and thus

$$\dot{V} = \frac{1}{L^2}\int_0^1 \left[-|k_T|\, w(t,x) - k\right] w_x^2(t,x)\, dx. \tag{14}$$

The next step will be a case–by–case analysis investigating stability for different values of $w(t,x)$. Out of (14) it can be seen that $\dot{V} \leq 0$ if

$$-|k_T|\, w(t,x) - k \leq 0 \tag{15}$$

$$\Rightarrow w(t,x) \geq \frac{k}{-|k_T|}. \tag{16}$$

A. Case 1: $w(t,x) \geq 0$

The first case denotes freezing, meaning that u / $\overline{T}$ is smaller than $T(t,x)$. This case is automatically fulfilled in the requirement formulated in (16).

B. Case 2: $w(t,x) \leq 0$

The second case describes thawing, meaning that u / $\overline{T}$ is bigger than $T(t,x)$. Here the bound on u has to be regarded: 235 K $\leq u \leq$ 255 K. This case requires a deeper study of the term $\frac{k}{-|k_T|}$ whose plot can be seen in Fig. 7.

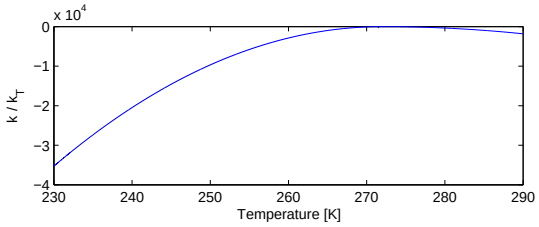

Fig. 7. Plot of $\frac{k}{-|k_T|}$ over temperature

Here the worst case scenario is described by $\overline{T} = 255$ K and $T(t,x) = 235$ K leading to a maximal negative error $w(t,x) = -20$ °C. The highest reachable temperature for this case is the upper bound to the input and thus a maximal value $\frac{k(255\text{ K})}{-|k_T(255\text{ K})|} = -5782.7$ is obtained fulfilling (16).

Hence it is shown that inequality (15) is fulfilled for the definitions of the parameters k_T and k, u bounded and all possible values of $w(t,x)$. With this knowledge *Poincaré's inequality* (see [10, Eq. 2.30]) can be introduced to (14) with a bound $\overline{K}$ representing the left hand side of (15) and consequently the PDE (1) is asymptotically stable:

$$\dot{V} \leq -\frac{\overline{K}}{4L^2}\int_0^1 w^2(t,x)\, dx := -\frac{\overline{K}}{4L^2}\|w(t)\|^2 = -\frac{\overline{K}}{4L^2} V.$$

IV. OPTIMIZATION PROBLEM

The continuous, nonlinear model (12) imposes constraints to the optimal control problem (OCP). The spatial discretization resolution was chosen to be $N = 25$. With N uneven, the exact center of the discretized space can be defined, namely $n = 13$. After simulation with a constant input function $u = 235$ K, τ is set to 6000 s. The objective function is chosen to be a least squares tracking term (LSQ) with constant reference values.

Thus, the formulation of the OCP looks as follows

$$\underset{u}{\textit{minimize}} \quad \int_0^{\tau} \left(T_i - T_{ref,i}\right)^T Q \left(T_i - T_{ref,i}\right) + R\left(u - u_{ref}\right)^2 dt$$

subject to

$$\begin{aligned} & T(0) = T_{init} \\ & \text{Discretized model (12) with the} \\ & \quad \text{boundary conditions } T_0 = T_{N+1} = u \\ & \underline{u} \le u \le \overline{u} \\ & \text{Terminal constraints (see appendix)} \end{aligned} \tag{17}$$

where $T_{ref,i}$ describes a vector containing the constant reference temperatures for the i-th state, u_{ref} is a scalar representing the reference input temperature, τ denotes the time horizon for the OCP, Q is a positive definite diagonal matrix that suits the size of $\left(T_i - T_{ref,i}\right)$ containing weights on state deviations, R is a scalar representing the weights on input deviations, T_{init} indicates the initial temperature and $\underline{u}$ and $\overline{u}$ are the lower and upper bounds to the input temperature, respectively. The values for these parameters and the terminal constraints are listed in the appendix. Note that the temperature references $T_{ref,i}$ correspond with the upper values for the terminal constraints $T_i(\tau)$, and these values are chosen to be largest in the core of the fish block and become lower towards the boundary. This is done to assure that the interior of the fish block is frozen below 255 $K \mathrel{\widehat{=}} -18$ °C so that there is a temperature margin for the outer layers when the fish block is being further distributed to the storage freezer. Note further that there are no path constraints defined for states and inputs.

A. Solving method

To solve the OCP a direct single shooting approach is chosen, where a predefined time horizon τ gets divided into a fixed time grid $0 = t_0 < t_1 < \cdots < t_G = \tau$ (not equidistant). Between each of the time instances a piecewise constant input function gets chosen and implemented into the ODEs. Then the set of ODEs, now only depending on the states, gets integrated by using a Runge Kutta method of order 7/8 with relative tolerance of 10^{-8}. After input discretization and numerical ODE solution, a Nonlinear Program (NLP) is obtained which is solved by Sequential Quadratic Programming (SQP). The approximation of the Hessian matrix in the SQP solver is chosen as Gauss-Newton. The tolerance level for the KKT conditions is set to 10^{-2}.

B. Software

The optimization software ACADO provides a MATLAB interface with automatic C++ code generation and is used here. With ACADO, different optimal control problems can be solved, such as offline dynamic optimization, parameter and state estimation as well as combined online estimation and MPC. For a deeper view of the structure and the principles behind ACADO, please see [9], [3] and [2]. In the latter two it is well-described how to formulate an OCP in ACADO/MATLAB.

V. SIMULATIONS AND RESULTS

The state plots only show T_1 to T_{13} due to the symmetry of the system. The same input function acts similarly on both boundaries and thus $T_{14} = T_{12}$, $T_{15} = T_{11}$, and so on.

To be able to have a reference to the obtained solution of the OCP, a simulation with constant input $u = 235$ K is shown in Fig. 8. Note the constant temperature values around $T = 272$ K due to the earlier described phenomenon of latent heat of fusion.

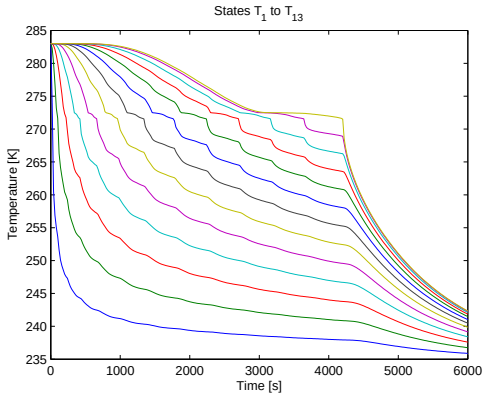

Fig. 8. Simulation with constant input u: States T_1 to T_{13}

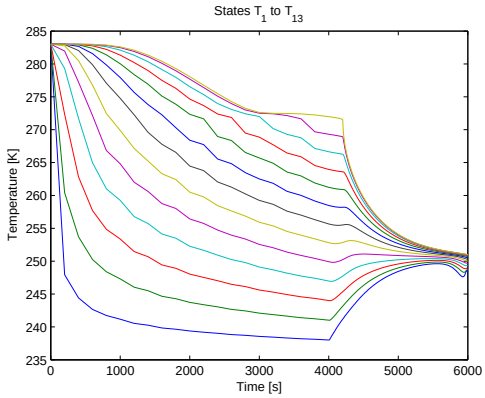

Fig. 9. States T_1 to T_{13}

In Fig. 9 and 10 the solution to the OCP (17) for the time grid vector $[0:200:4000 \quad 4005:5:6000]$ (421 time instances) is presented. The vector gets chosen like this after a series of a simulations showed that in the beginning the lower bound on the input function is active for about 4000 s. Then the input function changed and therefore the time grid vector was adapted to smaller step sizes.

The increase of temperature close to the boundary is due to the increase in the input function and despite this increase the interior of the fish block is still frozen down due to the cold front moving through it.

In Fig. 11 the temperature distribution at $\tau = 6000$ s is shown over the whole spatial direction x. The peaks on the boundaries result from the optimal solution (see overshoot

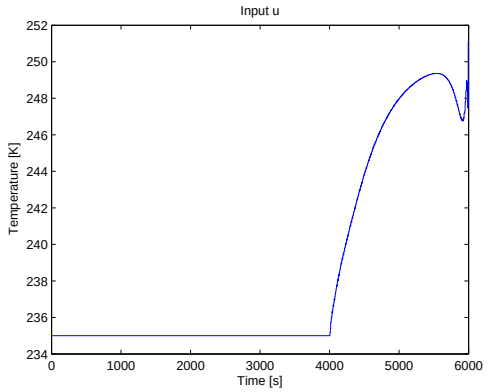

Fig. 10. Input u

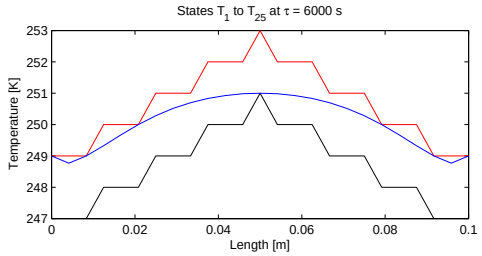

Fig. 11. Temperature distribution at $\tau = 6000$ s (blue) with upper and lower bounds to the terminal constraints (red and black) and $T_{ref,i}$ (red)

of the input function in Fig. 10 just before $\tau = 6000$ s). One can easily see that the terminal constraints are fulfilled.

VI. CONCLUSION AND FUTURE WORK

In this paper a solution to an optimal control problem for the heat equation with phase change taking latent heat of fusion into account has been found. The solution for the input function (Fig. 10) is a series of step functions. A smooth function can be found to approximate this optimal solution, but will most likely lead to a suboptimal solution.

However, the piecewise constant input function makes this approach not directly implementable. In future work a new state variable limiting the slope of the input function could be introduced to the OCP. Thus the temperature dynamics of the ammonia could be taken into account more accurately.

REFERENCES

[1] Nils Altmüller and Lars Grüne. Distributed and boundary model predictive control for the heat equation. Technical report, University of Bayreuth, Department of Mathematics, 2012.

[2] David Ariens, Moritz Diehl, Hans Joachim Ferreau, Boris Houska, Filip Logist, and Milan Vukov. *ACADO Toolkit User's Manual*. Optimization in Engineering Center (OPTEC) and Department of Electrical Engineering, K. U. Leuven, version 1.0.2613beta edition, June 2011.

[3] David Ariens, Hans Joachim Ferreau, Boris Houska, and Filip Logist. *ACADO for Matlab User's Manual*. Optimization in Engineering Center (OPTEC) and Department of Electrical Engineering, K. U. Leuven, Leuven, Belgium, version 1.0beta - v2022 edition, June 2010.

[4] Christoph Josef Backi and Jan Tommy Gravdahl. Modeling of the freezing process for fish in vertical plate freezers. In *Proceedings of the 17th Nordic Process Control Workshop*, Copenhagen, Denmark, 2012.

[5] Moritz Diehl. *Script-Draft: Numerical Optimal Control*. June 2011.

[6] Stevan Dubljevic and Panagiotis D. Christofides. Predictive control of parabolic pdes with boundary control actuation. *Chemical Engineering Science*, 61:6239–6248, 2006.

[7] Stevan Dubljevic, Nael El-Farra, Prashant Mhaskar, and Panagiotis D. Christofides. Predictive control of parabolic pdes with state and control constraints. *International Journal of Robust and Nonlinear Control*, 16:749–772, 2006.

[8] Michael Hinze, Rene Pinnau, Michael Ulbrich, and Stefan Ulbrich. *Optimization with PDE Constraints (Mathematical Modelling: Theory and Applications)*. Springer, 2009.

[9] Boris Houska, Hans Joachim Ferreau, and Moritz Diehl. Acado toolkit - an open-source framework for automatic control and dynamic optimization. *Optimal Control Applications and Methods*, 32:298–312, 2011.

[10] Miroslav Krstic and Andrey Smyshlyaev. *Boundary control of PDEs: A course on backstepping designs*. SIAM, 2008.

[11] Mohamad Muhieddine, Édouard Canot, and Ramiro March. Various approaches for solving problems in heat conduction with phase change. *International Journal of Finite Volume Method*, 6(1), 2008.

[12] Jorge Nocedal and Stephen J. Wright. *Numerical Optimization*. Springer Series in Operations Research, second edition, 2006.

[13] Q. Tuan Pham. A fast, unconditionally stable finite-difference scheme for heat conduction with phase change. *International Journal of Heat and Mass Transfer*, 28:2079–2085, 1985.

[14] Q. Tuan Pham. Mathematical modeling of freezing processes. In *Handbook of Frozen Food Processing and Packaging*, chapter 7. Taylor & Francis Group, LLC, 2006.

[15] Q. Tuan Pham. Modelling heat and mass transfer in frozen foods: a review. *International Journal of Refrigeration*, 29:876–888, 2006.

APPENDIX

TABLE I

SIMULATION PARAMETERS

L	0.1	m
LH	280000	Jkg^{-1}
N	25	[-]
T_f	272	K
T_{init}	283	K
ΔT	0.5	K
Δx	0.004	m
c_s	2200	$\mathrm{Jkg}^{-1}\mathrm{K}^{-1}$
c_l	3800	$\mathrm{Jkg}^{-1}\mathrm{K}^{-1}$
$\underline{u}$	235	K
$\overline{u}$	255	K
ρ	950	kgm^{-3}
λ_s	1.8	$\mathrm{Wm}^{-1}\mathrm{K}^{-1}$
λ_l	0.5	$\mathrm{Wm}^{-1}\mathrm{K}^{-1}$
τ	6000	s

TABLE II

LSQ PARAMETERS

Q	$0.1 \cdot \mathrm{I}_{(25x25)}$
R	0.01
$T_{ref,1..25}$	[249 249 249 250 250 250 251 251 251 252 252 252 253 252 252 252 251 251 251 250 250 250 249 249 249] K
u_{ref}	255 K

TABLE III

TERMINAL CONSTRAINTS

$247\ \mathrm{K} \leq T_{1,2,3,23,24,25}(\tau) \leq 249\ \mathrm{K}$
$248\ \mathrm{K} \leq T_{4,5,6,20,21,22}(\tau) \leq 250\ \mathrm{K}$
$249\ \mathrm{K} \leq T_{7,8,9,17,18,19}(\tau) \leq 251\ \mathrm{K}$
$250\ \mathrm{K} \leq T_{10,11,12,14,15,16}(\tau) \leq 252\ \mathrm{K}$
$251\ \mathrm{K} \leq T_{13}(\tau) \leq 253\ K$